Lip Tracking Using Particle Filter and Geometric Model for Visual Speech Recognition

Islem Jarraya[1], Salah Werda[2] and Walid Mahdi[1]
[1]*Multimedia InfoRmation systems and Advanced Computing Laboratory (MIRACL), ISIMS, University of Sfax, route de Tunis Km 10, Sfax, Tunisia*
[2] *Multimedia InfoRmation systems and Advanced Computing Laboratory (MIRACL), ISGI, University of Sfax, route de Tunis Km 10, Sfax, Tunisia*

Keywords: Lip Localization, Geometric Lip Model, Lip Tracking, Lip Descriptors Extraction, Viseme Classification and Recognition.

Abstract: The automatic lip-reading is a technology which helps understanding messages exchanged in the case of a noisy environment or of elderly hearing impairment. To carry out this system, we need to implement three subsystems. There is a locating and tracking lips system, labial descriptors extraction system and a classification and speech recognition system. In this work, we present a spatio-temporal approach to track and characterize lip movements for the automatic recognition of visemes of the French language. First, we segment lips using the color information and a geometric model of lips. Then, we apply a particle filter to track lip movements. Finally, we propose to extract and classify the visual informations to recognize the pronounced viseme. This approach is applied with multiple speakers in natural conditions.

1 INTRODUCTION

Speech is an effective means of communication used by speakers to understand and exchang messages. In fact, in noisy environments, the complex message can be more intelligible and better understood when it is accompanied by the vision of lip movements; it is the visual recognition of the speech. Many researches in the literature investigated their researches in this context, for example; (Sunil, 2013) and (Sunil, 2014). They seek to automate lipreading.

Several research works stressed their objectives in the research on modeling and tracking of the lips such as; (Mahdi, 2008) , (Cheung, 2011) (Stillittano, 2013) and (Sunil, 2013). Two types of approaches of segmentation have been used for lipreading: the low-level approach and The high level approach.

1.1 The Low-Level Approach (Image-based Approaches)

There are some researches that used the low segmentation techniques to detect the lip area such as; (Mahdi, 2008), (Bouvier, 2010), and (Kalbkhani, 2012). These approaches use directly the information present in the image of the mouth region and especially the pixel information. In practice, methods of this type allow rapid locations of the interest's zones but can not carry out a precise detection of the lip edges.

1.2 The High Level Approach (Model-based Approaches)

There are some researches using the high segmentation techniques such as; (Mahdi, 2008), (Liu, 2011), (Stillittano, 2013) and (Sunil, 2013) use the high level approach to detect the lip area. These approaches use a deformable model and integrate regularity constraints. There are two different types of deformable models which are used; active contours and parametric models.

1.2.1 Active Contours

There are some researchers that used active contours such as; (Sunil, 2013) and (Liu, 2011). Active contour has great flexibility to extract complex contours. However, when the environmental conditions are noisy, the detection of the true edge is not always guaranteed.

Jarraya I., Werda S. and Mahdi W..
Lip Tracking Using Particle Filter and Geometric Model for Visual Speech Recognition.
DOI: 10.5220/0005045601720179
In *Proceedings of the 11th International Conference on Signal Processing and Multimedia Applications* (SIGMAP-2014), pages 172-179
ISBN: 978-989-758-046-8

1.2.2 Parametric Models

There are some researchers that used parametric models such as; (Mahdi, 2008), and (Stillittano, 2013). The main advantage offered by parametric models is the integration of a priori knowledge about the shape. This benefit helps the model to converge good contours.

In order to automatically recognize visemes (visual phoneme), we must implement a system to extract relevant visual features on the lips of the speaker. Therefore, we must develop a system for locating and tracking mouth to characterize the lip movements.

This paper is organized as follows. Section (1) includes the introduction. In section (2), we are going present our proposed method. Section (3) will contains the evaluation of the concerned method and we present our rates of viseme recognition. Finally, section (4) is for the conclusion.

2 PROPOSED METHOD

We followed the same stages as proposed by (Mahdi, 2008) for the recognition of visemes, so our proposed method contains three successive stages. The first stage includes the lip localization. In the second stage we use the particle filter for lip tracking. The third stage we extracted the visual descriptors for the recognition of visemes.

In this paper tracking the movements of the lips is the principal objective. In fact, we need to consider a state vector p_t compound of parameters that characterize the state of the initial object. To make this vector, it is necessary to locate and segment the lips in the step of initialization at time *t=0*.

2.1 Localization of the Closed Mouth

We use two successive thresholding to localize the mouth. The first threshold is applied to detect the region of the face. The second threshold is applied to detect the region of the mouth.

According to (Beaumesnil, 2006), the Red component is always predominant whatever the color of the skin. Thus, we used the RGB space to detect the face and lip areas. But, the presence of the light in this space is very high. Actually, the normalization of the RGB space by the luminance component Y reduces the effect of light in the image. We tested two different equations luminance defined by the equation (1) and equation (2) (Mahdi, 2008).

$$Y1 = R + G + B \quad (1)$$

$$Y2 = 0.299 * R + 0.587\, G + 0.114 * B \quad (2)$$

The first thresholding is to detect pixels that contain the dominance of the Red component compared to the Green and Blue components in the normalized image $R_nG_nB_n$. This is summarized in the following program:

```
if ( Rn(i,j) > Gn(i,j) et Rn(i,j) > Bn(i,j))
      P(i,j) = 0
else
      P(i,j) = 255
```

The result obtained by thresholding is presented in Figure 1.

(a) (b) (c)

Figure 1: Face detection; (a) Source image, (b) Facial area after thresholding and normalization with Y1, (c) Facial area after thresholding and normalization with Y2.

The difference between the Red and Green components is greater for the lips than the skin (Nicolas, 2003). Thus, we think that this difference can be a chromatic variable $X_i = (R_n - G_n)_i$ used for segmenting lips (i is the number of pixels of the facial area).

In Figure 2, we show the variation of the difference between the two components Red and Green of the facial area. We define a dynamic threshold to detect only the areas that correspond to the upper part of the great peaks of the curve where the Red color is more dominant (equation (3) with $\bar{X}_i$: The average of all X_i, $\delta(X_i)$: Deviation of all X_i). Figure 2 illustrates the detection of these great peaks with the dynamic threshold.

$$\text{Threshold} = \bar{X}_i + \delta(X_i) \quad (3)$$

The second threshold results a labial localization (See Figure 3). We try to clean the result of the last threshold to move near the true lip area. Thus, we use a morphological filter in order to delete false pixels detected in the skin.

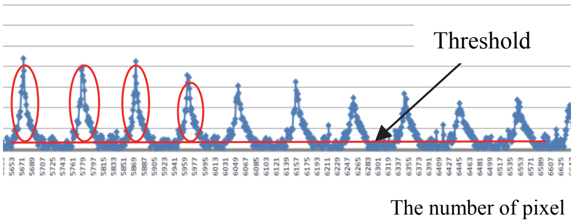

Figure 2: Curve obtained from the difference between the red color and the green color of the face area.

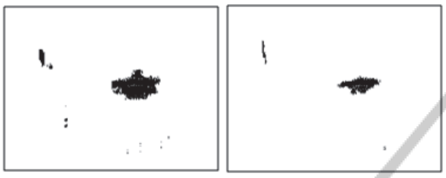

(a) (b)

Figure 3: Detection lip; (a) the result is obtained after the application of the second threshold with the image of Figure 1(b), (b) the result is obtained after the application of the second threshold with the image of Figure 1(c).

According to (Mahdi, 2008), the corners of the mouth (right (Cd) and left (Cg)) are defined as the right and left ends of the center (C) (See Figure 4). They are detected by using the combination of the saturation and gradient information. This method of detection is more explained in (Mahdi, 2008). In effect, these two corners are the parameters of initialization, which are used to create a geometric model that exploits a priori knowledge about the shape of the lips (Figure 4) (Mahdi, 2008). This model is composed of three curves: the curve y_{11} and y_{12} to trace the contour of the upper lip (Equation (4), Equation (5)) and the curve y_2 to trace the contour of the lower lip (Equation (6)).

$$y_{11} = -\frac{(-\beta_1 + 2\alpha_1\beta_1 + x^2\beta_1 + 2x\alpha_1\beta_1)}{(-2\alpha_1 + \alpha_1{}^2 + 2x\beta_1\varepsilon_1 + 2\beta_1\alpha_1\varepsilon_1 + 1)} \quad (4)$$

$$y_{12} = \frac{(\beta_1 + 2\alpha_1\beta_1 + x^2\beta_1 + 2x\alpha_1\beta_1)}{(-2\alpha_1 + \alpha_1{}^2 + 2x\beta_1\varepsilon_1 + 2\beta_1\alpha_1\varepsilon_1 + 1)} \quad (5)$$

$$y_2 = \frac{(\beta_2 - (x^2)^{\alpha_2} * \beta_2)}{(2 * \alpha_2 * \beta_2 * \varepsilon_2 - 1)} \quad (6)$$

The parameters β, α and ε offer flexibility to cover the lips (See Figure 4). The β parameter represents the height of a sub model. The parameter α describes the degree of curvature of the model. The ε parameter allows some tolerance for asymmetrical lips.

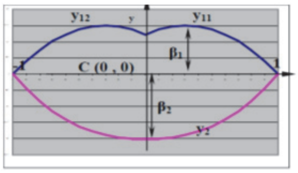

Figure 4: Geometric model (Mahdi, 2008).

The tracing of the lip contour is done by creating a number of possibilities models and selecting the model that correspond to the most important external energy of the gradient image (Mahdi, 2008). Figure 5 represents the tracing of the geometric model that adapts the lip contour.

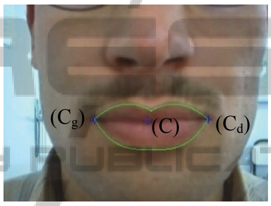

Figure 5: Lip contour.

2.2 Tracking Lip Contour by the Geometric Model

The corners are the initialization parameters of the geometric model. This allows us to propose that every evolution and deformation of the model are related to the moving of the corners position over time. Therefore, lip contour tracking by the geometric model is linked to corners tracking.

In our case, we use the particle filter for lip tracking. This filter is a set of advanced predictive techniques based on simulation. It used in several works to track a linear or no linear specific object such as; (Shirinzadeh, 2012), (Majumdar, 2013), (Segura, 2014) and (Meng, 2014), etc.

2.2.1 Tracking of Corners

Using the particle filter, at time *t=0*, the two corners (right C_d and left C_g) of the initial geometric model M_0 are considered as initial objects ($(C_0)_d$ and $(C_0)_g$). Then the state vector "p_t" of these objects contains two pose parameters 2D ($C_t = [p_t]^T = [x_t, y_t]^T$). These parameters are the spatial coordinates. Using the principle of dynamic model $P(x_t|x_{t-1})$, n of the predictive corners are created according to equation (7). (n is experimentally defined)

$$C_t = \hat{C}_{t-1} + U_t \tag{7}$$

The object "$\hat{C}_{t-1}$" has undergone random transitions by adding a random vector U_t. This vector has a normal distribution *N(0,K)* with a transitional distance equal to "*K*" that is experimentally defined.

In the evaluation step, each particle is defined by a block of pixel neighborhoods of size *N* * *N* pixels. To calculate the weight of each particle we use the the manhattan distance between the initial corner C_0 at time "*t = 0*" and the particle which are shown in grayscale. This distance measure the degree of difference between the two intensity vectors of the neighborhoods pixels of the particle and the pixels of the initial corner C_0. Equation (8) defines this distance (x_j : the neighborhoods pixels *j* of the particle *i* at time "*t*", y_j: the neighborhoods pixels *j* of the initial corner C_0, the pixel x_j corresponds the pixel y_j).

$$D = \sum_{j=1}^{N} |x_j - y_j| \tag{8}$$

Thus, the weight W_t^i of the particle C_t^i is the similarity *S* between the particle and the object C_0. The equation (9) defines this measure (W_t^i: the weight of the particle *i* at time "*t*", C_t^i: the particle *i* at time "*t*", C_0: the initial corner). To estimate the optimal object, we keep only the ten particles which have the highest weight. Then, we calculate the Euclidean distance $d(C_t^i|\hat{C}_{t-1})$ between the position of the particle C_t^i and the position of the optimal corner of the time "*t-1*" $\hat{C}_{t-1}$. Thus, the selected particle has the most similarity (the most weight) and the smallest Euclidean distance. (Equation (10)).

$$W_t^i = S(C_t^i|C_0) = 1/D \tag{9}$$

$$\hat{\pi}_t^i = max \left\{ \begin{matrix} S\left((C_t^i)\middle|(C_0)\right) \\ + 1/\, d(C_t^i|\hat{C}_{t-1}) \end{matrix} \right\}_{i=1}^{10} \tag{10}$$

2.2.2 Tracking Lip Contour

At time "*t=0*", the geometric model that represents the lip contour M_0 is considered as the initial object. At each time "*t*", using the principle of dynamic model *P(M_t|M_{t-1})*, we predict *n* particles depending on the selected corners $(C_t)_g$ and $(C_t)_d$ and the state of the selected model $\widehat{M}_{t-1}$ at time "*t-1*" ($\widehat{M}_{t-1}$ is the optimal model at time "*t-1*" and *n* is experimentally defined) (See Figure 6).

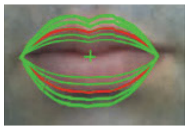

Figure 6: Tracing *n* particles (green) around the selected model (red) at time "*t-1*".

The coordinates of the two corners right $(C_t)_d$ and left $(C_t)_g$ are noted $((x_t)_d, (y_t)_d)$ and $((x_t)_g, (y_t)_g)$. Then, generated particles M_t^i are linked of poses data (x_t^i, y_t^i) with $i \in [1, \dots, n]$, $x_t^i \in [(x_t)_d, (x_t)_g]\ \forall\, t$ and $y_t^i = M_t^i = \{(y_{11})_t^i, (y_{12})_t^i, (y_2)_t^i\}$ (Equation (11), Equation (12), Equation (13), Equation (14)). In fact, y_t^i is linked of six parameters $(\beta_1)_t^i$, $(\beta_2)_t^i$, $(\alpha_1)_t^i$, $(\alpha_2)_t^i$, $(\varepsilon_1)_t^i$ et $(\varepsilon_2)_t^i$. Thus, at time "*t*", the state vector of the selected model $\widehat{M}_{t-1}$ is noted by $[p_{t-1}]^T = [(\beta_1)_{t-1}^i, (\beta_2)_{t-1}^i, (\alpha_1)_{t-1}^i, (\alpha_2)_{t-1}^i, (\varepsilon_1)_{t-1}^i, (\varepsilon_2)_{t-1}^i]^T$.

$$M_t^i = \begin{cases} (y_{11})_t^i \\ (y_{12})_t^i \\ (y_2)_t^i \end{cases} \tag{11}$$

$$(y_{11})_t^i = \frac{-(-{\beta_1}_t^i + 2{\alpha_1}_t^i\,{\beta_1}_t^i + x^2{\beta_1}_t^i}{\dfrac{(-2{\alpha_1}_t^i + {\alpha_1}_t^{i\,2} + 2x{\beta_1}_t^i\,{\varepsilon_1}_t^i + 2x{\alpha_1}_t^i\,{\beta_1}_t^i)}{+ 2{\beta_1}_t^i\,{\alpha_1}_t^i\,{\varepsilon_1}_t^i + 1)}} \tag{12}$$

$$(y_{12})_t^i = \frac{({\beta_1}_t^i + 2{\alpha_1}_t^i\,{\beta_1}_t^i + x^2{\beta_1}_t^i}{\dfrac{(-2{\alpha_1}_t^i + {\alpha_1}_t^{i\,2} + 2x{\beta_1}_t^i\,{\varepsilon_1}_t^i + 2x{\alpha_1}_t^i\,{\beta_1}_t^i)}{+ 2{\beta_1}_t^i\,{\alpha_1}_t^i\,{\varepsilon_1}_t^i + 1)}} \tag{13}$$

$$(y_2)_t^i = \frac{\left({\beta_2}_t^i - (x^2)^{{\alpha_2}_t^i} * {\beta_2}_t^i\right)}{\left(2 * {\alpha_2}_t^i * {\beta_2}_t^i * {\varepsilon_2}_t^i - 1\right)} \tag{14}$$

Each parameter has undergone a random transformation by adding a random vector U_t. We assume that this vector has a normal distribution *N(0,K)* with a transitional distance equal to "*K*" that is experimentally defined. The transformation of the parameters is as follows: $(\beta_1)_t = \widehat{\beta_1}_{t-1} + U_t$, $(\beta_2)_t = \widehat{\beta_2}_{t-1} + U_t$, $(\alpha_1)_t = \widehat{\alpha_1}_{t-1} + U_t$, $(\alpha_2)_t = \widehat{\alpha_2}_{t-1} + U_t$, $(\varepsilon_1)_t = \widehat{\varepsilon_1}_{t-1} + U_t$ and $(\varepsilon_2)_t = \widehat{\varepsilon_2}_{t-1} + U_t$. In point of fact, $\widehat{\beta_1}_{t-1}$, $\widehat{\beta_2}_{t-1}$, $\widehat{\alpha_1}_{t-1}$, $\widehat{\alpha_2}_{t-1}$,

$\hat{\varepsilon}_{1_{t-1}}$ and $\hat{\varepsilon}_{2_{t-1}}$ are parameters of the optimal model $\widehat{M}_{t-1}$ at time "*t-1*".

In the evaluation stage, we define *m* points on the initial geometric model and their corresponding *m* points on each particle. (*m* is experimentally defined) In our case *m* equal 14 (See Figure 7).

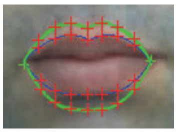

Figure 7: Tracing *m* points on the initial geometric model (blue) and *m* points on the particle (green).

Each point is defined by a block of neighborhoods pixel of size *N* * *N*. To calculate the weight W_t^i of each particle, we use the Manhattan distance *D* between two intensity vectors of neighborhoods pixels of the point *j* (*j* ∈*[1, ..., m]*) of the initial model and pixels of the corresponding point in the particle. Thus, the similarity *S* of a particle is equal to the inverse of the sum of the manhattan distances between the *m* points of the initial model M_0 and their corresponding points of the particle M_t^i (*i*∈*[1, ..., n]*) (Equation (15)).

To estimate the optimal object, we keep only the ten particles which have the highest weight, and we calculate the Euclidean distance $d(M_t^i|\widehat{M}_{t-1})$ between the position of the particle M_t^i (*i*∈*[1, ..., n]*) and the position of the optimal model of the time "*t-1*" $\widehat{M}_{t-1}$. Thus, the selected particle has the most similarity (the most weight) and the smallest Euclidean distance. (Equation (16)).

$$W_t^i = S\left(M_t^i \middle| M_0\right) = 1/\sum_{j=1}^{m} D \tag{15}$$

$$\hat{\pi}_t = max\{S\left(M_t^i \middle| M_0\right) + 1/d(M_t^i|\widehat{M}_{t-1})\}_{i=1}^{10} \tag{16}$$

2.3 Lip Feature Extraction

The choice of the syllabic descriptors must be relevant and accurately describe the movement of each viseme in a corpus. According to (Mahdi, 2008), the most relevant descriptors are visual descriptors (See Figure 8):

- The horizontal distance between lip corners (DH)
- The vertical distance between the lower and the upper lip (DV')
- The vertical distance between the lower lip and the centre of the mouth (DV'')
- The degree of the opening mouth (Opening Degree: OD)
- The dark surface (Dark Area: DA) inside the mouth
- The teeth surface (Tooth Area: TA).

In fact, we add two new descriptors (See Figure 8):

- The lip surface (Lip Area: LA)
- The lip position (Lip Position: LP) (the spatial position of the lip pixels of the mouth).

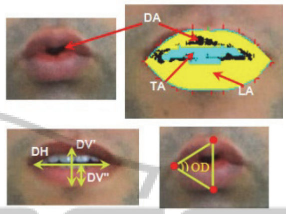

Figure 8: Different descriptors characterizing the lip movements.

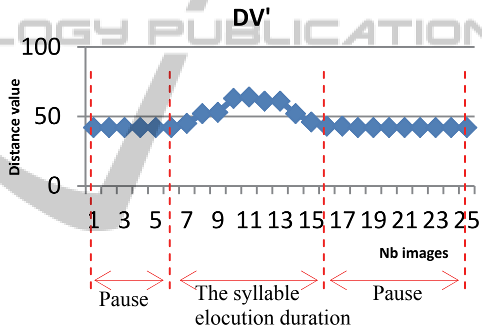

Figure 9: Tracking of DV' with syllable /ba/.

The variation of each descriptor during the syllabic sequence constructed a data vector. This vector is the input information in the learning phase for the visual recognition of the pronounced viseme.

We note that there are two periods of silence at the beginning and at the end of the speech sequence. We use DV' to detect these periods because this descriptor describes the start and the end of lip movements (Figure 9). According to (Mahdi, 2008), the two periods of silence will be ignored for all the descriptors, in order to not influence the final recognized template. Then, we propose to apply a spatial-temporal normalization on the tracking curves. The normalization is to provide a representation of the different tracking curves by the same number of images (w) and in the same range of values between 0 and 1.

The elocution sequence is captured with 25 frames/s (fps). Moreover, According to (Mahdi, 2008), who used all the frames consecutively for the duration of 0.4 seconds. Then, in our case, (w) is fixed to 10.

2.4 Viseme Corpus Presentation

We used the corpus of (Mahdi, 2008). This corpus is composed of 40 native speakers, of various age and sex. It has been created in natural conditions. The capture is done with one CCD camera; the resolution is 0.35 Mega of pixels and with 25 frames/s (fps). This cadence is widely enough to capture the major important lip movement (Mahdi, 2008).

In the French language, we can see three differentiable lip movements for vowels: group A (Opening movement), group O (Forward movement) and group I (Stretch movement). Thus, our corpus consists of syllable sequences for three visemes (/ba/, /bi/, /bou/) that are visually differentiable. These visemes cover three lip movements: /ba/ for opening /bi/ for stretching and /bou/ for the forward movement.

3 EXPERIMENTAL RESULTS

We present in this section three experimental parts. In the first part, we evaluate our lip localization method, in the second part, we evaluate our lip tracking method and the third part is used for the experimentation and the evaluation of our system for the visual recognition of each viseme present in our corpus.

3.1 Evaluation of Our Localization Method

In order to present the result of the location of the mouth, we draw the detected center of the lip area. In fact, the step of lip localization is more important to create the lip contour

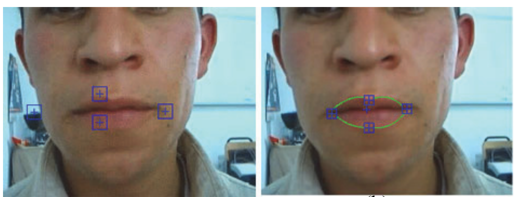

(a) (b)

Figure 10: Experimental Results for different speakers (create the lip contour and detect the four POI “Points Of Interest: the two corners, the lower point of the lower lip and the upper point of the upper lip”): (a) results of (Mahdi, 2008), (b) our results.

If the center of the mouth is bad positioned, the corners may be poorly positioned and the detection of the lip contour becomes difficult.

In (Mahdi, 2008) there is a single threshold to detect the mouth by searching the area where the Red component is dominant ($R_n > R_n$ and $G_n > B_n$). Figure 10 shows a comparison between the results of lip localization and lip segmentation with results of (Mahdi, 2008).

3.2 Evaluation of Our Tracking Method

Figure 11 presents the results of tracking and extracting of the lip movement and the lip descriptors.

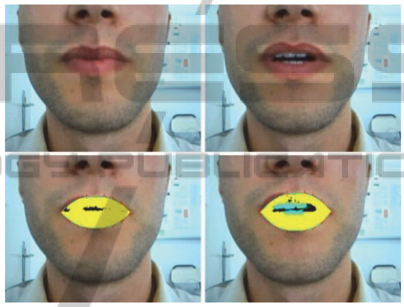

Figure 11: Track and extraction of lip movement and lip descriptors: pronunciation of the viseme /ba/.

In order to evaluate our tracking method, we propose to compare our results with the found results of (Mahdi, 2008). Figure 12 shows a comparison of some experimental results. The comparison with found results by the vote algorithm of (Mahdi, 2008) shows that there is an improvement in tracking using the particle filter.

In order to properly assess the tracking method, we try another comparison with manual tracking (a more real tracking). So, we consider in this part that the automatic and manual trackings are based on the evolution of the four points POI of the mouth. The four POI are the right and left corner, the Up POI (The upper point of the upper lip) and the Down POI (the lower point of the lower lip) (Figure 13).

First, we manually detect the positions of the POI in each frame of 45 sequences using "Matlab R2010a" software. Then, the position of POI is automatically calculated again from the automatic tracking of lip contour. Finally, our tracking method is evaluated by a comparison between automatic and manual POI tracking. This comparison is determined by extracting the mistake of POI tracking. This mistake is defined by the Euclidean distance between the POI spatial coordinates which is determined by using the manual and the automatic tracking. Tracking errors of 45 sequences are represented by “Table 1”.

Figure 12: Tracking of lip movement: (a) (b) followed by vote algorithm of (Mahdi, 2008), (c) (d) followed by our method (filter particles).

Figure 13: The four points POI of the mouth.

Average errors POIs are varied in the interval [0.9 pixels, 1.8 pixels] “Table 1”. We note that the error of tracking is not very important. This argues the robustness of our tracking method.

Table 1: Tracking error in 45 sequences for three visemes (/ba/, /bi/ and /bou/).

	Error value (pixels)	
	Average	Deviation
Right corner	0,9625	0,5697
Left corner	0,8812	0,6629
Up POI	1,0648	0,6543
Down POI	1,8125	1,2742

3.3 Viseme Recognition

Training and visual recognition require the division of our audiovisual corpus into two parts. We have used 70% of the corpus for stage training and 30% for recognition. We test the recognition percentage with two types of kernel SVM; the RBF and the polynomial. The percentage of recognition with the SVM of RBF kernel is equal to 82.8571% but with the polynomial kernel we obtain a percentage equal to 88.5714%. So we choose to represent the found experimental results with the SVM of polynomial kernel.

In order to test the utility of the two new descriptors "LA" and "LP", we test the recognition rate with four different cases (See “Table 2”).

Table 2: Experimental results found with the SVM of polynomial kernel and with three different cases of training.

	Recognition Rate			
	Without LA and LP	With LA and Without LP	Without LA and with LP	With LA and LP
/Ba/	58.33%	66.66%	83.33%	91.66 %
/Bi/	81.81%	81.81%	81.81%	81.81 %
/Bou/	91.66%	91.66%	91.66%	91.66 %
Recogni-tion Rate	77.14%	80%	85.71%	88.57 %

In “Table 2”, we note that the descriptors “LA” and “LP” affect the recognition of the viseme /ba/. In fact, according to the experimental results, the rate of confusion of the viseme /ba/ with the viseme /bi/ is reduced by adding these two descriptors. The histogram in Figure 14 shows the decrease of this confusion. Descriptors LA and LP characterize stretching movement of the lips when pronounce the viseme /bi/. So this viseme becomes more identifiable.

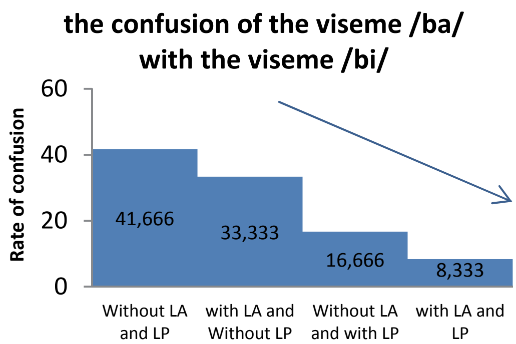

Figure 14: Experimental results of viseme confusion.

In order to properly evaluate the recognized results, the following table shows a comparison with the results of recognition of (Mahdi, 2008) (See “Table 3”).

Comparing our results with the results of (Mahdi, 2008), we find that our recognition rates are higher than recognition rates found by (Mahdi, 2008). This result shows that our system of tracking and characterization of lip movements contributes to improve visual recognition of visemes.

Table 3: Experimental results are found with the SVM of polynomial kernel and with three different cases of training.

	Recognition Rate (Mahdi, 2008)	Recognition Rate (Our method)
/Ba/	72.73%	91.66%
/Bi/	90.91%	81.8181%
/Bou/	81.82%	91.6666%
Recognition Rate	81.82%	88.57%

4 CONCLUSIONS

Systems of visual recognition of the speech require visual descriptors. So, to extract these descriptors, it is necessary to make a localizing and an automatic tracking of the labial gestures.

Our objective is to provide a method for segmenting the labial area and to tracking and characterizing the lip movements with the best possible precision to achieve better recognition of visemes.

In this paper, we presented early our segmentation method to extract the outer contour of the lips. Then, we track the lip contour using the particle filter and extract lip descriptors throughout the syllable sequence. Finally we chose the SVM method for training and recognition of visemes. This approach has been tested with success on our audiovisual corpus.

Our lip-reading system can be improved by integrating many new perspectives. In fact, we plan to expand the content of our corpus by adding others visemes, different words and even phrases from different languages. We can also add audio information.

REFERENCES

Beaumesnil, B., 2006. Real Time Tracking for 3D Realistic Lip Animation. In *ICPR, International Conference Pattern Recognition*. IEEE.

Bouvier, C., 2010. *Segmentation Region-Contour des contours des lèvres*. Prepared in the laboratory GIPSA-lab/DIS within the Graduate School Electronics, Electrotechnics, Automation & Signal Processing Laboratory of Computer Vision and Systems Université Laval.

Kalbkhani, H., Amirani, M., 2012. An Efficient Algorithm for Lip Segmentation in Color Face Images Based on Local Information. In *JWEET'01, Journal of World's Electrical Engineering and Technology*. Science-line.

Liu, X., Cheung Y., 2011. A robust lip tracking algorithm using localized color active contours and deformable models.In *ICASSP, IEEE International Conference on Acoustics, Speech and Signal Processing*.IEEE.

Mahdi, W., Werda, S., Ben Hamadou, A., 2008. A hybrid approach for automatic lip localization and viseme classification to enhance visual speech recognition.In *ICAE'03, Integrated Computer-Aided Engineering*. ACM.

Majumdar, J., Kiran, S., 2013. Particle Filter Integrating Color Model for Tracking. In *IJETAE'07, International Journal of Emerging Technology and Advanced Engineering*.

Meng, J., Liu, J., Zhao, J., Wang, J., 2014. Research of Real-time Target Tracking Base on Particle Filter Framework. In Jofcis'06. *Journal of Computational Information Systems*. Binary Information Press.

Nicolas, E., 2003. *Segmentation des lèvres par un modèle déformable analytique*. Prepared at the Laboratory of Images and Signals (LIS) within the Doctoral School.

Segura, C., Hernando, J., 2014. 3D Joint Speaker Position and Orientation Tracking with Particle Filters. In *Sensors'02. Sensors and Transducers Journal*. MDPI.

Shirinzadeh, F., Seyedarabi, H., Aghagolzadeh, A., 2012. Facial Features Tracking Using Auxiliary Particle Filtering and Observation Model Based on Bhattacharyya Distance. In *IJCTE'05. International Journal of Computer Theory and Engineering*. EBSCO.

Stillittano, S., Girondel, V., Caplier, A., 2013. Lip contour segmentation and tracking compliant with lip-reading application constraints. In *Mach. Vis. Appl.'01. Proceedings of Mach. Vis. Appl*. Springer-Verlag.

Sunil, M., Patnaik, S., 2013. Automatic Lip Tracking and Extraction of Lip Geometric Features for Lip Reading. In *IJMLC'02. International Journal of Machine Learning and Computing*. IACSIT.

Sunil, M., Patnaik, S., 2014. Lip reading using DWT and LSDA. In *IACC. IEEE International Advance Computing Conference* . IEEE.